Available online at www.sciencedirect.com
ScienceDirect
Journal of Nuclear Materials 363–365 (2007) 786–790
journal of nuclear materials
www.elsevier.com/locate/jnucmat

Simulation of divertor pumping in JT-60U with SOLDOR/NEUT2D code

H. Kawashima *, K. Shimizu, T. Takizuka, N. Asakura, H. Takenaga, T. Nakano, S. Sakurai

Japan Atomic Energy Agency, 801-1, Mukoyama, Naka, Ibaraki 311-0193, Japan

Abstract

To characterize the divertor pumping for particle and heat control in the SOL/divertor and to extrapolate to future devices, simulations using the SOLDOR/NEUT2D code are performed on the JT-60U experiment. The simulation reproduces fairly well the neutral pressure and pumping flux in the exhaust chamber. A parametric survey shows that the pumping efficiency η_{pump} (ratio of pumping flux to generated flux around the divertor targets) increases with the pumping speed. It is found that a pumping speed higher than the present capability (26 m^3/s) is necessary for the active particle control under the wall saturation condition. When the strike-point distance is shortened from 10 to 2 cm, the η_{pump} is enlarged by a factor of 1.5 with increase of the slot view angle. A virtual tilt of the divertor targets to 15° vertically enhances η_{pump} by a factor of 1.2 and leads simultaneously to a lower target heat load.

PACS: 52.25.Ya; 52.40.Hf; 52.55.Fa; 52.65.Pp

Keywords: Divertor simulation; JT-60U; Divertor pumping; Particle control

1. Introduction

In order to predict the particle and heat controllability in the tokamak divertor for future devices, numerical simulations are required. For the design study of the ITER divertor, modeling codes such as B2-EIRENE [1], UEDGE [2] and EDGE2D [3] have been used.

In the Japan Atomic Energy Agency (JAEA), a SOL/divertor code SOLDOR/NEUT2D has been developed for the interpretation and the prediction of the behavior of plasmas and neutrals in the SOL/divertor [4,5]. The code development is carried out since physics models can be verified and modified quickly and flexibly with close collaboration with the JT-60 team.

Recently, the divertor pumping is treated as a significant issue. Experimental results for long pulse discharges in JET [6] and JT-60U [7,8] showed confinement degradation in the latter phase of the discharges with a density increment. The wall pumping became ineffective due to the saturation of the wall inventory. In such a condition for future tokamak reactors, the divertor pumping plays a

* Corresponding author. Fax: +81 29 270 7419.
E-mail address: kawashima.hisato@jaea.go.jp (H. Kawashima).

0022-3115/$ - see front matter
doi:10.1016/j.jnucmat.2007.01.127

crucial rule in the particle and heat control for high-β steady-state operation.

In this paper, we perform simulations of the divertor pumping in the JT-60U long pulse discharges under wall saturation conditions by using the SOLDOR/NEUT2D code. The pumping efficiency (defined later) characterizes the pumping capability with dependence on the pumping speed and strike-point distance.

2. SOLDOR/NEUT2D code

The SOLDOR/NEUT2D code couples the 2D plasma fluid code SOLDOR with the neutral Monte Carlo (MC) code NEUT2D. Fine meshes ($\leqslant$2 mm) are used around the divertor targets as seen in Fig. 1 with consideration of the short mean free path of neutral particles (a few mm in dense divertor plasmas). The neutral particle transport is solved inside the vessel including the exhaust structure in order to evaluate accurately the neutral influx into those boundaries. Various collision processes between neutral and plasma particles are treated in the NEUT2D code [5]. The MC noise is reduced by introducing the 'piling' method [5], and the performance of NEUT2D is optimized on the massive parallel computer, SGI ALTIX 3900. As a result, the steady-state solution can be obtained within a computational time of 3–4 h.

For simulations on the JT-60U experiments, the plasma boundary in the SOLDOR code is set at $r/a = 0.95$. Total power and ion fluxes (Q_{total}, Γ_{ion}) across $r/a = 0.95$ are given as input parameters. The carbon contamination is set to 2% of deuterium density. A simplified non-coronal model [9] with a residence parameter $n_e\tau_{\text{res}} = 4 \times 10^{15}$ s/m^3 is applied for the carbon impurity radiation. The recycling of deuterium is assumed to be 100% at the first wall. The pumping speed is specified by an albedo for neutrals at the entrance of the pumping port. Drifts in the SOL are not considered. Under these conditions, the neutral transport and the plasma transport in the SOL/divertor are simulated self-consistently with assuring the convergence to a steady state by careful treatment of the particle balance between SOLDOR and NEUT2D codes.

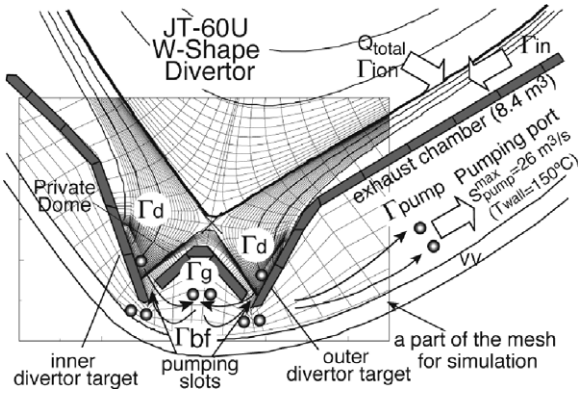

Fig. 1. Schematic view of divertor pumping system in the JT-60U tokamak. A part of mesh for SOLDOR/NEUT2D calculation is also shown.

3. Simulation of divertor pumping in JT-60U

Fig. 1 shows the divertor pumping system in the JT-60U tokamak. Neutral particles through the inner and outer pumping slots are exhausted into the outer pumping port by the cryo-pump system. The total pumping speed is 26 m^3/s at the temperature of the first wall of 150 °C. Simulations are performed along the experiments on the pumping speed, the supplied fluxes (wall desorption and gas puffing) and the strike point distance. Particle fluxes {Γ_{ion}: ion flux at the core boundary ($r/a = 0.95$), Γ_{in}: supplied neutral fluxes (wall fuelling Γ_{wall}, and gas puff Γ_{puff}), Γ_{d}: generated neutral flux around the divertor targets, Γ_{g}: neutral flux into exhaust chamber through slots, Γ_{bf}: neutral back-flow from the exhaust chamber, Γ_{pump}: pumping flux} are defined in the figure for analyses of the simulation results.

3.1. Dependence of pumping efficiency on pumping speed

A JT-60U neutral-beam (NB) heated long pulse discharge (35 s) with $I_p/B_t = 1.2$ MA/2 T in the lower-single-null configuration was performed under the wall saturation condition [8]. The injected NB power P_{NBI} is 4 MW, which corresponds to a particle fuelling rate of $\sim 0.4 \times 10^{21}$ s^{-1}. Fig. 2(a) shows time evolutions of the supplied fluxes Γ_{puff}, Γ_{wall}, neutral pressure P_0 (measured by a penning gauge) and pumping flux Γ_{pump} in the exhaust chamber, and so on. The pumping speed S_{pump} was increased from 10 to 26 m^3/s at $t = 20$ s by opening the fast shutters at the pumping ports. After $t = 20$ s, P_0 was reduced and Γ_{pump} was increased by the increase of S_{pump}. On the other hand, the main plasma density (line averaged electron density n_e in the figure) and divertor recycling were changed little. This constancy is possibly kept

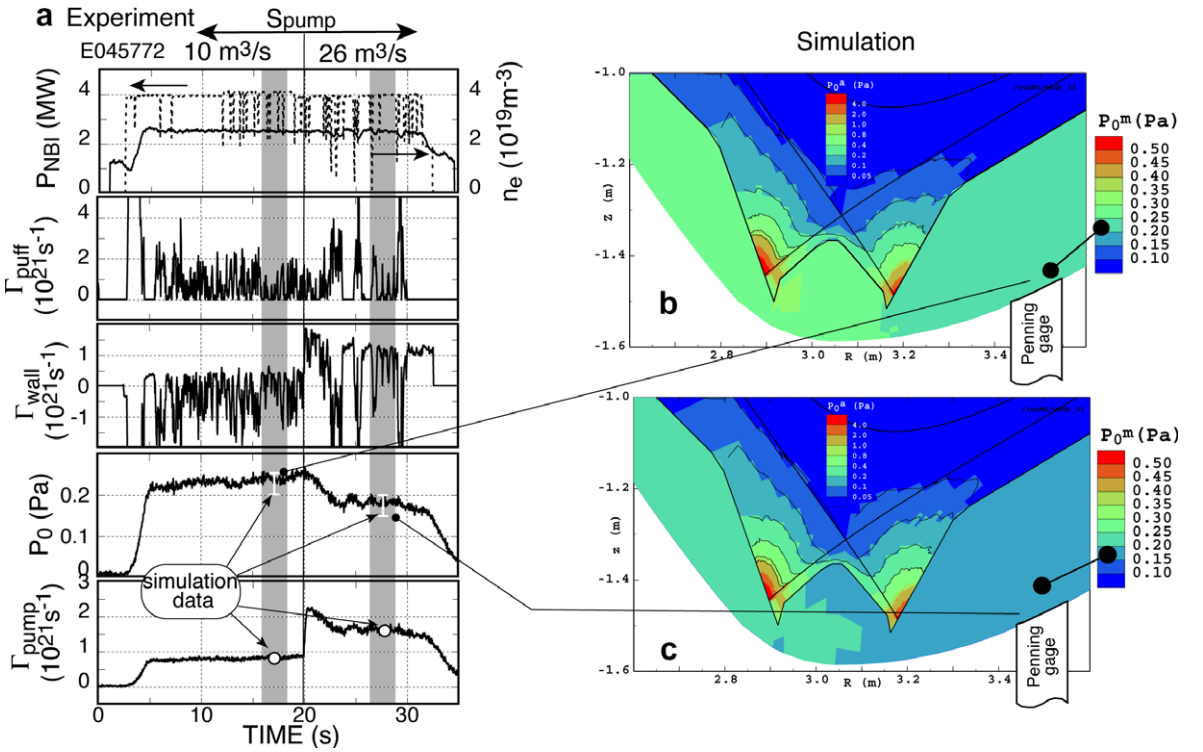

Fig. 2. (a); Time evolutions of P_{NBI}, n_e, Γ_{puff}, Γ_{wall}, P_0, and Γ_{pump}, when the pumping speed is increased from 10 to 26 m^3/s at $t = 20$ s in the JT-60U long pulse discharge under wall saturation conditions. (b) and (c) Simulated contour plots of neutral pressure (molecular pressure in the exhaust chamber and atom pressure in the divertor region) for (b) $S_{pump} = 10$ m^3/s and (c) $S_{pump} = 26$ m^3/s.

by the increase of the extra fuelling by the wall desorption ($\Gamma_{wall} > 0$) after $t = 20$ s with response to the pumping speed.

Simulations of the divertor pumping are carried out for the discharge in Fig. 2(a). The input parameters are chosen as $Q_{total} = 3.8$ MW and $\Gamma_{ion} = 1.4 \times 10^{21}$ s^{-1} according to the experimental conditions of input power and edge density. We assume a particle diffusion coefficient $D = 0.3$ m^2/s and a thermal electron and ion diffusivity $\chi^e_\perp = \chi^i_\perp = 1$ m^2/s based on the empirical values for various tokamaks [10]. To simulate the steady phases around $t = 17$ s ($S_{pump} = 10$ m^3/s) and $t = 27$ s ($S_{pump} = 26$ m^3/s) (hatched regions in Fig. 2(a)), the supplied experimental neutral fluxes Γ_{in} ($=\Gamma_{wall} + \Gamma_{puff}$) in each phase are given as 0.6×10^{21} s^{-1} and 1.5×10^{21} s^{-1}. Fig. 2(b) and (c) show the simulation results of the neutral pressure distribution. The distribution profile in the divertor plasma region changes only a little, while the neutral pressure in the exhaust chamber P_0 decreases for (c) $S_{pump} = 26$ m^3/s. The calculated values of P_0 and Γ_{pump} for both cases agree very well with experimental values as indicated in Fig. 2(a). Simultaneously, the simulated heat loads on the divertor targets form an in/out asymmetry and both peak values are close to those measured by the infrared camera system. The sum of the integrated heat load (total power received on the targets) and the total radiation loss power in the divertor region almost equals Q_{total}, meaning that the heat balance is satisfied consistently. For both cases of $S_{pump} = 10$ and 26 m^3/s, the heat load profile changes little as well as the neutral pressure in the divertor plasma region (Fig. 2(b) and (c)) and the plasma density.

The dependence of the pumping efficiency η_{pump} on the pumping speed is evaluated by expanding the capacity based on results above. Here η_{pump} (as an index of the pumping capability) is defined as the ratio of Γ_{pump} to Γ_d; $\eta_{pump} \equiv \Gamma_{pump}/\Gamma_d = (\Gamma_g/\Gamma_d) \cdot (1 - \Gamma_{bf}/\Gamma_g)$ [5,11]. Fig. 3(a) and (b) show the dependences of η_{pump} and Γ_d on S_{pump}, respectively, for various Γ_{in} values. The η_{pump} increases with the increase of S_{pump} and Γ_{in}. In Fig. 3(b) two simulation points for the experiment of Fig. 2 are marked. At these two points the pumping speed

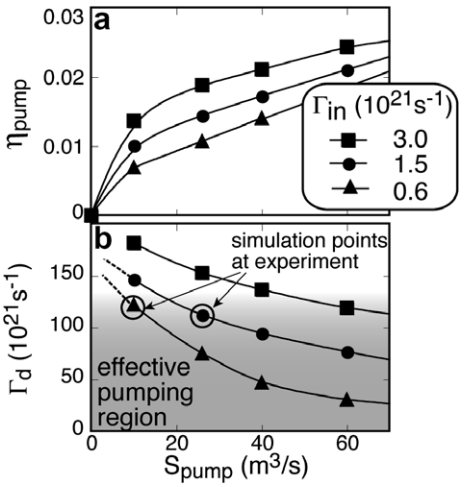

Fig. 3. Dependences of (a) η_{pump} and (b) Γ_d on S_{pump} as a function of Γ_{in}.

affects little the main and divertor plasmas, because the increased Γ_{pump} is balanced with the extra wall fuelling ($\Gamma_{wall} > 0$). Although the particle controllability depends on the amount of Γ_{wall} (unknown factor), it is found that higher η_{pump} or S_{pump} in the hatched region in Fig. 3(b) is required at least for an active particle control under the wall saturation conditions. It is future work to find how the plasma condition can be controlled with consideration of the wall fuelling.

3.2. Dependence of pumping efficiency on strike point distance

In order to characterize the divertor pumping, the distance (L_{in}, L_{out}) from the dome wing extension point on the target to the strike point of the separatrix (called 'strike-point distance') was changed for two cases: (a) (averaged distance on inner/outer sides $L_{ave} = 2$ cm) and (b) ($L_{ave} = 4.3$ cm) in Fig. 4 at the experiments. The results showed that the Γ_{wall}, P_0 and Γ_{pump} in case (a) became larger than those in case (b), while the main plasma density was unchanged similar as in the experiment in Fig. 2(a). It suggests that the pumping became effective with neutral compression by approaching the strike point to the pumping slot. For the simulation, the η_{pump} dependence on the strike-point distance is evaluated for four cases by adding the case (c) ($L_{ave} = 7.5$ cm) and case (d) ($L_{ave} = 10$ cm) as shown in Fig. 4. The input parameters are the same as those for the simulation for the case of $S_{pump} = 26\ m^3/s$ in Fig. 2. The η_{pump} is increased by shortening the distance, contrasting with a reduction of Γ_d (Fig. 5). This can also be found from the calculated fluxes (Table 1), which leads an enhancement of the incident fraction Γ_g/Γ_d (meaning a

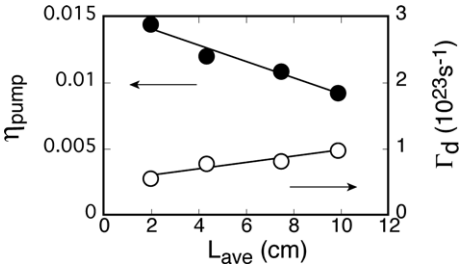

Fig. 5. Dependences of η_{pump} and Γ_d on the strike-point distance.

Table 1
Relations among neutral fluxes (Γ_d, Γ_g, Γ_{bf}, Γ_{pump}) four cases in Fig. 4

	L_{ave} (cm)	Γ_d (10^{23} s^{-1})	Γ_g/Γ_d	Γ_{bf}/Γ_g	η_{pump}
Case (a)	2	0.56	0.29	0.95	0.0145
Case (b)	4.3	0.78	0.24	0.95	0.0120
Case (c)	7.5	0.83	0.21	0.95	0.0109
Case (d)	10	0.98	0.17	0.94	0.0093

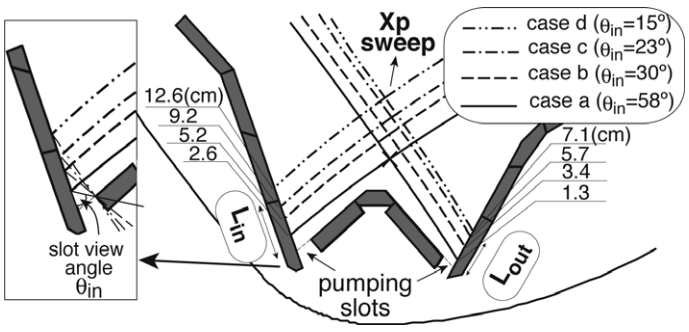

Fig. 4. Schematic view when the strike-point distance is changed at four cases. Slot view angle θ_{in} increases with shortening the distance.

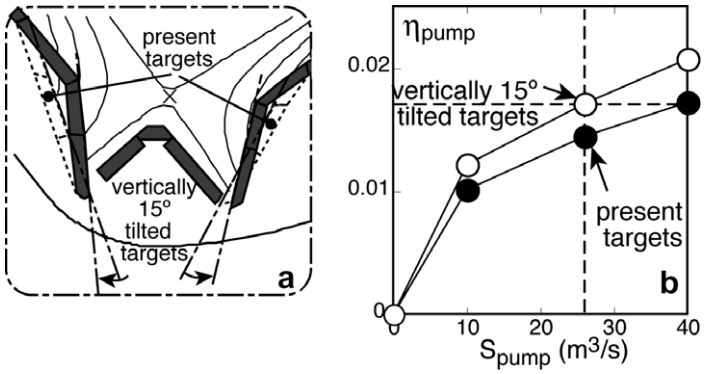

Fig. 6. (a) Schematic views of virtual tilt of 15° and present divertor targets. (b) Comparison of η_{pump} as a function of S_{pump}.

degree of neutral compression) by increasing the slot view angle θ_{in}.

4. Discussions

Tilting the divertor target vertically can reduce the divertor heat loads as was shown in the divertor design study for the JT-60NCT (now JT-60SA) [11]. Besides, the above pumping effect studies make an anticipation to improve the pumping capability by such modification. From this viewpoint in the simulations, the divertor targets in JT-60U are virtually tilted 15° vertically and the pumping efficiency is compared with that for the present geometry (Fig. 6(a) and (b)). The pumping slot width ~3 cm is kept as before by a minor modification of private dome. The input parameters are the same as in Fig. 2. The pumping efficiency on the tilted target is clearly improved. The η_{pump} at $S_{pump} = 26\ m^3/s$ becomes almost the same as that at $S_{pump} = 40\ m^3/s$ in the present configuration. Although the limitation in the plasma equilibria must be considered, it is found that the vertically tilted target is possibly favorable from the viewpoint of high pumping capability and low heat loads for future devices.

5. Conclusion

Using the SOLDOR/NEUT2D code, a simulation of the divertor pumping is performed for a JT-60U long pulse discharge under wall saturation conditions. The simulation reproduces fairly well the neutral pressure and pumping flux in the exhaust chamber by treating the desorbed flux from the wall similar as the gas puff flux. The heat loads on the divertor targets satisfy the heat balance consistently. Based on this result, we evaluated the dependences of the pumping efficiency η_{pump} ($\equiv \Gamma_{pump}/\Gamma_d$) on the S_{pump} and L_{ave}. It clearly shows that η_{pump} increases with an increase of S_{pump}. While, results both of experiments and simulations showed that the particle balance in the present pumping capacity owed by the amount of Γ_{wall}, which indicates that higher η_{pump} or S_{pump} is required to improve the particle controllability with independent of Γ_{wall}. On the other hand, by a shortening of the L_{ave} from 10 to 2 cm, the η_{pump} is enlarged by a factor of 1.5 due to an increase of the fraction of incident flux into the exhaust chamber via a larger slot view angle. By a virtual tilt of the divertor targets to 15° vertically, η_{pump} is enhanced by a factor of 1.2 with a low target heat load, providing a favorable possibility for future devices.

Acknowledgements

The authors are grateful to the members of the JT-60 team for their supports and fruitful discussions. This work is partly supported by a Grant-in-Aid for Scientific Research of Japan Society for the Promotion of Science.

References

[1] R. Schneider et al., J. Nucl. Mater. 196–198 (1992) 810.
[2] T.D. Rognlien et al., J. Nucl. Mater. 196–198 (1992) 347.
[3] R. Simonini et al., J. Nucl. Mater. 196–198 (1992) 369.
[4] K. Shimizu et al., J. Nucl. Mater. 313–316 (2003) 1277.
[5] H. Kawashima et al., Plasma Fusion Res. 1 (2006) 031.
[6] J. Jacquinot et al., Plasma Phys. Control. Fusion 35 (1993) A35.
[7] H. Takenaga et al., J. Nucl. Mater. 337–339 (2005) 802.
[8] T. Nakano et al., Nucl. Fusion 46 (2006) 626.
[9] D.E. Post, J. Nucl. Mater. 220–222 (1995) 143.
[10] ITER Physics Basis, Chapter 4: Power and particle control, Nucl. Fusion 39 (1999) 2391.
[11] H. Kawashima et al., Fusion Eng. Des. 81 (2006) 1613.